Inorg. Chem. **1984**, *23*, 2519–2528

Contribution from the Department of Chemistry, La Trobe University, Bundoora, Victoria 3083, Australia,
and Department of Physical and Inorganic Chemistry, University of Adelaide, Adelaide, South Australia 5001, Australia

Synthesis and Characterization of Complexes of Thiomolybdates and Thiotungstates with Copper(I) and Silver(I) Cyanides, Including ^{95}Mo and ^{183}W NMR Properties and the Crystal and Molecular Structures of (n-Pr$_4$N)$_2$[(CN)CuS$_2$MoS$_2$], (n-Pr$_4$N)$_2$[(CN)AgS$_2$WS$_2$], and (Ph$_4$As)$_2$[(CN)CuS$_2$MoS$_2$Cu(CN)]·H$_2$O

STEPHEN F. GHELLER,[1a] TREVOR W. HAMBLEY,[1b] JOHN R. RODGERS,[1b] ROBERT T. C. BROWNLEE,[1a]
MAXWELL J. O'CONNOR,*[1a] MICHAEL R. SNOW,*[1b] and ANTHONY G. WEDD*[1a]

Received September 13, 1983

Polymeric (NH$_4$)CuMoS$_4$ is cleaved by aqueous cyanide. Addition of quaternary cation A$^+$ allows isolation of A$_2$[(CN)CuS$_2$MoS$_2$] and, in the presence of 1 equiv of CuCN, of A$_2$Cu$_2$(CN)$_2$MoS$_4$·H$_2$O, which contains the discrete [(CN)CuS$_2$MoS$_2$Cu(CN)]$^{2-}$ anion for A = Ph$_4$As. More generally, addition of M′CN (M′ = Cu, Ag) to aqueous solutions of [MS$_4$]$^{2-}$ (M = Mo, W) generates [(CN)M′S$_2$MS$_2$]$^{2-}$ and [(CN)M′S$_2$MS$_2$M′(CN)]$^{2-}$, while [(CN)M′S$_2$MOS]$^{2-}$ is formed in solutions of [MOS$_3$]$^{2-}$. The crystal structures of (n-Pr$_4$N)$_2$[(CN)CuS$_2$MoS$_2$] and (n-Pr$_4$N)$_2$[(CN)AgS$_2$WS$_2$] reveal the presence of discrete, binuclear dianions, [(CN)M′S$_2$MS$_2$]$^{2-}$, of C_{2v} point symmetry with a MS$_4$ group acting as a bidentate ligand to an essentially linear M′CN unit. The major variations in the detailed structures are consistent with the difference in sizes of the Cu and Ag atoms. The crystal structure of (Ph$_4$As)$_2$[(CN)CuS$_2$MoS$_2$Cu(CN)]·H$_2$O contains discrete, trinuclear dianions of close to D_{2d} symmetry in which the MS$_4$ group acts as a bidentate ligand to each of two CuCN units. The water molecule is disordered over two sites, about 0.6 Å apart, which are both within hydrogen-bonding distance of the cyanide nitrogen atoms. This structure contrasts with the polymeric nature of the salt (Me$_4$N)$_2$(CN)$_2$Cu$_2$MoS$_4$ examined previously. The electronic spectra of the cyanide complexes are dominated by the internal transitions of the [MS$_4$]$^{2-}$ and [MOS$_3$]$^{2-}$ ligands, modified by the effects of lower symmetry. A systematic examination of the ^{95}Mo and ^{183}W NMR of the metalate anions [MO$_{4-n}$X$_n$]$^{2-}$ (X = S, Se) has been made. A systematic decrease in shielding of the metal nuclei occurs with successive substitution of ligand oxygen by sulfur or selenium. The downfield shift is respectively 497–604 ppm per S and 658–873 ppm per Se in [MoO$_{4-n}$X$_n$]$^{2-}$ in aqueous solution while the corresponding range for [WO$_{4-n}$S$_n$]$^{2-}$ is 841–1009 ppm. The solvent dependence of the chemical shift of [MoS$_4$]$^{2-}$ is pronounced, being over 70 ppm in the solvents examined. The resonances for the cyanide complexes are all shielded relative to the parent metalate anions. A striking feature for all the compounds examined is the constant ratio of chemical shifts $\delta(^{183}\mathrm{W}):\delta(^{95}\mathrm{Mo}) = 1.67 \pm 0.3$, which can be compared with the value 1.7 observed previously for substituted carbonyl species of very different chemical nature. The ^{95}Mo NMR line widths are dependent upon rotational correlation time, site symmetry, and the presence of neighboring quadrupolar nuclei ^{63,65}Cu. Crystal data for (n-Pr$_4$N)$_2$[(CN)CuS$_2$MoS$_2$]: a = 9.712 (1) Å, b = 12.686 (3) Å, c = 14.474 (2) Å, α = 76.07 (1)°, β = 83.98 (1)°, γ = 81.19 (1)°, triclinic, $P\bar{1}$, Z = 2. Crystal data for (Ph$_4$As)$_2$[(CN)CuS$_2$MoS$_2$Cu(CN)]·H$_2$O: a = 9.561 (2) Å, b = 15.158 (3) Å, c = 18.027 (2) Å, α = 97.45 (1)°, β = 101.30 (1)°, γ = 91.81 (2)°, triclinic, $P\bar{1}$, Z = 2. Crystal data for (n-Pr$_4$N)$_2$[(CN)AgS$_2$WS$_2$]: a = 9.546 (3) Å, b = 13.009 (2) Å, c = 14.692 (2) Å, α = 75.62 (1)°, β = 84.93 (2)°, γ = 80.57 (2)°, triclinic, $P\bar{1}$, Z = 2.

Introduction

Various aspects of the chemistry of the simple thioanions of molybdenum(VI) and tungsten(VI), [MO$_{4-n}$S$_n$]$^{2-}$ (n = 1–4), are currently being examined[2–5] and are proving to be intriguingly complex. While the high metal oxidation state is stabilized by the strong σ- and π-donor properties of the oxo and sulfido ligands, the anions are very reactive. Both the MO and MS linkages are susceptible to electrophilic attack (particularly protonation[6]) while the latter can also undergo nucleophilic attack (by cyanide,[2] for example). Both processes can lead to condensation reactions that are complicated by the highly developed redox properties of the metals and of sulfide. Consequently, a burgeoning series[2,7a] of polythiometalates is emerging that features reduced metal oxidation states and oxidized sulfur ligands such as S$_2$$^{2-}$. Under more highly reducing conditions, the sulfido ligand is maintained. For example, in the presence of *excess* thiolate, the reaction of [MS$_4$]$^{2-}$ with Fe$^{\mathrm{III}}$ sources leads[3] to the assembly of [M$_2$Fe$_6$S$_8$(SR)$_9$]$^{3-}$ and related anions containing "cubane" [Fe$_3$MS$_4$] fragments. However, the fascinating interplay of metal, sulfide, and thiolate redox potentials is highlighted by the following reaction[7b] where *both* the metal and disulfide are formally reduced by metal-bound sulfide:

$$2[\mathrm{MoS_4}]^{2-} + \mathrm{RSSR} + 2\mathrm{H}^+ \rightarrow [\mathrm{Mo^V{}_2S_4(S_2)_2}]^{2-} + 2\mathrm{RSH}$$

Another facet of the chemistry of the thiometalate anions is their ligand properties.[2] They bond to a wide variety of metal centers M′ via the sulfur atoms, so acting as bi- or tridentate ligands. The physical integrity of the [MO$_{4-n}$S$_n$]$^{2-}$ moiety is maintained. An important stabilizing factor is the ability of the ligands to delocalize electron density from M′ into low-lying empty d-based orbitals. The particular thiometalate involved is important in the present context of M′ = Cu$^{\mathrm{I}}$ and Ag$^{\mathrm{I}}$, as the latter metals have little tendency to bind the oxo functions. Consequently, different structures are observed for the trinuclear species [(Ph$_3$P)$_3$Cu$_2$(MoS$_4$)][2,8a] and [(Ph$_3$P)$_3$Cu$_2$(MoOS$_3$)]:[8b]

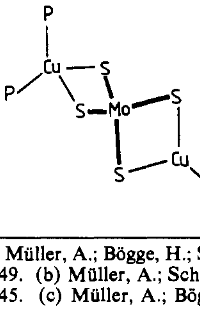

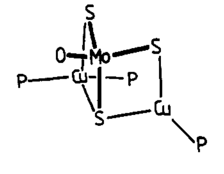

---

(1) (a) La Trobe University. (b) University of Adelaide.

(2) Müller, A.; Diemann, E.; Jostes, R.; Bögge, H. *Angew. Chem., Int. Ed. Engl.* **1981**, *20*, 934.

(3) Holm, R. H. *Chem. Soc. Rev.* **1981**, *10*, 455.

(4) Coucouvanis, D. *Acc. Chem. Res.* **1981**, *14*, 201.

(5) Wedd, A. G. In "Sulfur, Its Significance for Chemistry, the Geo-, Bio- and Cosmo-sphere and Technology"; Müller, A., Krebs, R., Eds.; Elsevier: Amsterdam, 1983; Vol. 4, p 181.

(6) Harmer, M. A.; Sykes, A. G. *Inorg. Chem.* **1980**, *19*, 2881.

(7) (a) Sechenesse, F.; Lefebvre, J.; Daran, J. C.; Jeannin, Y. *Inorg. Chim. Acta* **1981**, *54*, L175. (b) Harmer, M. A.; Pan, W.-H.; Halbert, T. R.; Stiefel, E. I. "Abstracts of Papers", 186th National Meeting of the American Chemical Society, Washington, DC, Aug 1983; American Chemical Society: Washington, DC, 1983.

(8) (a) Müller, A.; Bögge, H.; Schimanski, V. *Inorg. Chim. Acta* **1980**, *45*, L249. (b) Müller, A.; Schimanski, V.; Schimanski, J. *Ibid.* **1983**, *76*, L245. (c) Müller, A.; Bögge, H.; Schimanski, V. *Ibid.* **1983**, *69*, 5.

0020-1669/84/1323-2519$01.50/0

Other interesting clusters include tetranuclear species of varying structure such as $[(Ph_3P)_3Cu_3(MOS_3)Cl]$,[2,8c] $[Cl_3Cu_3(MoOS_3)]^{2-}$,[8b] and $[Cl_3Cu_3(WS_4)]^{2-}$[9] and the hexanuclear species $[(Ph_3P)_4M'_4(MOS_3)_2]$.[10] Such species are providing a chemical basis to assist interpretation of the Cu–Mo–S interaction in higher animals, where copper–thiomolybdate interactions appear relevant.[11]

The present paper details the synthesis of bi- and trinuclear complexes of $[MS_4]^{2-}$ and $[MOS_3]^{2-}$ (M = Mo, W) with CuCN and AgCN and includes structural characterization of the three title salts. Preliminary details of $[(CN)CuS_2MoS_2]^{2-}$ have been communicated.[12] Aspects of these systems have been examined by others, including structural features[13] and metathesis reactions with PhS^- to produce[14] $[(PhS)CuMoS_2]^{2-}$ and $[(PhS)CuS_2MoS_2Cu(SPh)]^{2-}$. In addition, the present work reports both the ^{95}Mo and ^{183}W NMR properties of the $[MoO_{4-n}X_n]^{2-}$ (X = S, Se) and $[WO_{4-n}S_n]^{2-}$ (n = 0–4) systems as well as those of the binuclear and trinuclear complexes whose syntheses are described herein. In particular, this is the first report of ^{183}W NMR applied to such systems.

In 1975, chemical applications of ^{95}Mo ($I = {}^5/_2$) and ^{97}Mo ($I = {}^5/_2$) NMR were initiated by Vold[15] who studied the protonation behavior of $[MoO_4]^{2-}$ in the pH range 7–12. Soon after, Lutz, Nolle, and their co-workers published the first[16a] of a series of papers[16] on the ions $[MoO_{4-n}S_n]^{2-}$ (n = 0–4). In particular, they assigned individual resonances[16b,f] and demonstrated[16e] the sensitivity of ^{95}Mo chemical shifts to subtle structural change by resolving resonances for the isotopomers $[^{95}Mo^{16}O_{4-n}{}^{18}O_n]^{2-}$ (n = 0–4) and $[^{95}Mo^{32}S_{4-n}{}^{34}S_n]^{2-}$ (n = 0, 1).

The first direct observation of ^{183}W ($I = {}^1/_2$) NMR in solution was reported[17] in 1974. Low resonance frequency (ca. 4.16 MHz), low receptivity (0.058 relative to ^{13}C), and long relaxation times can make direct observation difficult,[18a] and consequently the majority of the reported chemical shift data has been derived for systems where double or triple resonance techniques[19] are possible. However, narrow line widths and resolved spin–spin coupling has provided key structural information[20] for polyoxotungstate systems and amply rewarded the labor of direct observation.

Experimental Section

Synthesis. Distilled water and analytical reagent grade solvents were used. Microanalysis was performed by Bernhardt Analytische Laboratorien, Elbach, West Germany.

Bis(tetra-*n*-propylammonium) Cyano(tetrathiomolybdenio-*S*,*S'*)-cuprate(2−), $(n\text{-}Pr_4N)_2[(CN)CuS_2MoS_2]$ (I). A solution of KCN (0.64 g, 9.8 mmol) in H_2O (7 cm^3) was added to a suspension of $(NH_4)CuMoS_4$[21a] (3.0 g, 9.8 mmol) in H_2O (30 cm^3) to produce a deep red solution. A solution of $(n\text{-}Pr_4N)Br$ (5.2 g, 19.6 mmol) in H_2O (10 cm^3) was added dropwise, producing a red precipitate. The mixture was stirred for 15 min before the compound, which was washed with H_2O, EtOH, and ether and dried in air, was isolated; yield 4.35 g (65%). Recrystallization from 95% EtOH at 60 °C yields bright red crystals. The Ph_4As^+ and Et_4N^+ salts may be prepared in a similar manner. The compounds may also be prepared by combining equimolar aqueous solutions of $(NH_4)_2[MoS_4]$[21b] and $Cu(CN)_x]^{1-x}$ (produced by combining $CuSO_4{\cdot}5H_2O$ or CuCN with KCN) followed by the addition of 2–3 equiv of the quaternary cation.

Bis(tetra-*n*-propylammonium) Cyano(tetrathiotungstenio-*S*,*S'*)-cuprate(2−), $(n\text{-}Pr_4N)_2[(CN)CuS_2WS_2]$ (III). Solid $(NH_4)_2[WS_4]$[21b] (5.0 g, 14.4 mmol) was added directly to a suspension of CuCN (1.28 g, 14.4 mmol) and KCN (3.74 g, 57.4 mmol) in H_2O (40 cm^3). The mixture was stirred for 5 min and filtered. To the filtrate was added a solution of $(n\text{-}Pr_4N)Br$ (7.65 g, 28.7 mmol) in H_2O (10 cm^3) to produce a yellow precipitate, which was stirred for 5 min, filtered off, and washed with H_2O, cold EtOH, and ether before drying in air; yield 6.2 g (56%). Recrystallization from hot 95% EtOH yields yellow crystals.

The analogous silver compounds $(n\text{-}Pr_4N)_2[(CN)AgS_2MoS_2]$ and $(n\text{-}Pr_4N)_2[(CN)AgS_2WS_2]$ can be prepared similarly by utilizing a suspension of AgCN produced by combining $AgNO_3$ and KCN in H_2O.

Bis(tetraphenylarsonium) (μ-Tetrathiomolybdenio-*S*,*S'*:*S''*:*S'''*)-bis(cyanocuprate)(2−)–Water (1/1), $(Ph_4As)_2[(CN)CuS_2MoS_2Cu(CN)]{\cdot}H_2O$ (II). The suspension produced by combining $CuSO_4{\cdot}5H_2O$ (2.7 g, 10 mmol) and KCN (1.6 g, 25 mmol) in H_2O (20 cm^3) was added to a solution of $(NH_4)CuMoS_4$ (3.1 g, 10 mmol) and KCN (1.0 g, 15.4 mmol) in water (10 cm^3). The mixture was stirred for 20 min and filtered. A solution of Ph_4AsBr (9.9 g, 21.4 mmol) in H_2O (10 cm^3) was added to the filtrate, producing an immediate precipitate, which was filtered off, washed with H_2O, cold EtOH, and ether, and dried in air. The crude material was recrystallized from hot 95% EtOH to yield orange-red needles, yield 1.2 g (10%). The $n\text{-}Pr_4N^+$ and the Et_4N^+ salts of the same empirical formula may be prepared analogously.

Bis(tetra-*n*-propylammonium) (μ-Tetrathiotungstenio-*S*,*S'*:*S''*:*S'''*)bis(cyanocuprate)(2−)–Water (1/1), $(n\text{-}Pr_4N)_2[(CN)CuS_2WS_2Cu(CN)]{\cdot}H_2O$. Solid $(NH_4)_2[WS_4]$ (5.0 g, 14.4 mmol) was added directly to a warm, stirred mixture of CuCN (2.58 g, 28.8 mmol) and KCN (2.0 g, 30.7 mmol) in H_2O (50 cm^3). The red solution was stirred for 1 h (a shorter period leads to a product contaminated with $(n\text{-}Pr_4N)_2[(CN)CuS_2WS_2]$) and filtered. Addition of a solution of $(n\text{-}Pr_4N)Br$ (8.0 g, 30 mmol) in H_2O (20 cm^3) produced a yellow precipitate, which was filtered off, washed with H_2O, and dissolved in hot EtOH (100 cm^3). Undissolved orange material was filtered off. Evaporation produced the final product, which was washed with H_2O, cold EtOH, and ether before being dried under vacuum.

Bis(tetraethylammonium) Cyano(oxotrithiomolybdenio-*S*,*S'*)-cuprate(2−), $(Et_4N)_2[(CN)CuS_2MoOS]$. Solid $K_3[MoOS_3]Cl$[21c] (1.0 g, 2.8 mmol) was added directly to a stirred mixture of $CuSO_4{\cdot}5H_2O$ (0.69 g, 2.8 mmol) and KCN (0.54 g, 8.3 mmol) in H_2O (5 cm^3). After stirring for 5 min, a solution of Et_4NBr (1.5 g, 5.5 mmol) in

---

(9) Manoli, J.-M.; Potvin, C.; Sechenesse, F. *J. Chem. Soc., Chem. Commun.* **1982**, 1159.

(10) (a) Müller, A.; Bögge, H.; Hwang, T. K. *Inorg. Chim. Acta* **1980**, *39*, 71. (b) Doherty, R.; Hubbard, C. R.; Mighell, A. D.; Siedle, A. R.; Stewart, J. *Inorg. Chem.* **1979**, *18*, 2991. (c) Königer-Ahlborn, E.; Müller, A. *Angew. Chem., Int. Ed. Engl.* **1976**, *15*, 680. (d) Stalick, J. K.; Siedle, A. R.; Mighell, A. D.; Hubbard, C. R. *J. Am. Chem. Soc.* **1979**, *101*, 2903.

(11) (a) Mills, C. F.; Bremner, I. A. In "Molybdenum and Molybdenum-Containing Enzymes"; Coughlan, M., Ed.; Pergamon Press: Oxford, 1980; p 517. (b) Mills, C. F. *Philos. Trans. R Soc. London, Ser. B* **1979**, *288*, 51.

(12) Gheller, S. F.; Gazzana, P. A.; Masters, A. F.; Brownlee, R. T. C.; O'Connor, M. J.; Wedd, A. G.; Rodgers, J. R.; Snow, M. R. *Inorg. Chim. Acta* **1981**, *54*, L131.

(13) Müller, A.; Dartmann, M.; Römer, C.; Clegg, A.; Sheldrick, G. M. *Angew. Chem., Int. Ed. Engl.* **1981**, *20*, 1060.

(14) Acott, S. R.; Garner, C. D.; Nicholson, J. R.; Clegg, W. *J. Chem. Soc., Dalton Trans.* **1983**, 713.

(15) Vold, R. R.; Vold, R. L. *J. Magn. Reson.* **1975**, *19*, 365.

(16) (a) Kautt, W. D.; Krüger, H.; Lutz, O.; Maier, H.; Nolle, A. *Z. Naturforsch., A* **1976**, *31A*, 351. (b) Lutz, O.; Nolle, A.; Kroneck, P. *Ibid.* **1976**, *31A*, 454. (c) Lutz, O.; Nepple, W.; Nolle, A. *Ibid.* **1976**, *31A*, 1046. (d) Buckler, K. U.; Haase, A. R.; Lutz, O.; Müller, M.; Nolle, A. *Ibid.* **1977**, *32A*, 126. (e) Lutz, O.; Nolle, A.; Kroneck, P. *Z. Phys. A* **1977**, *282A*, 157. (f) Lutz, O.; Nolle, A.; Kroneck, P. *Z. Naturforsch. A* **1977**, *32A*, 505. (g) Kroneck, P.; Lutz, O.; Nolle, A. *Ibid.* **1980**, *35A*, 226.

(17) Sahm, W.; Schwenk, A. *Z. Naturforsch. A* **1974**, *29A*, 1763.

(18) Harris, R. K.; Mann, B. E., Eds. "NMR and the Periodic Table"; Academic Press: London, 1978: (a) 214; (b) 17.

(19) Andrews, G. T.; Colquhoun, I. J.; McFarlane, W.; Grim, S. O. *J. Chem. Soc., Dalton Trans.* **1982**, 2353 and references therein.

(20) (a) Acerete, R.; Hammer, C. F.; Baker, L. C. W. *J. Am. Chem. Soc.* **1979**, *101*, 267. (b) Gansow, O. A.; Ho, R. K. C.; Klemperer, W. G. *J. Organomet. Chem.* **1980**, *187*, C27. (c) Lefebvre, J.; Chauveau, F.; Doppelt, P.; Brevard, C. *J. Am. Chem. Soc.* **1981**, *103*, 4589. (d) Acerete, R.; Hammer, C. F.; Baker, L. C. W. *Ibid.* **1982**, *104*, 5384. (e) Domaille, P. J.; Knoth, W. H. *Inorg. Chem.* **1983**, *22*, 818. (f) Finke, R. G.; Droege, M. W. *Ibid.* **1983**, *22*, 1006.

(21) (a) Redman, M. J. *Inorg. Synth.* **1973**, *14*, 95. (b) McDonald, J. W.; Friesen, G. D.; Rosenhein, L. D.; Newton, W. E. *Inorg. Chim. Acta* **1983**, *72*, 205. (c) Müller, A.; Schulze, H.; Sievert, W.; Weinstock, N. *Z. Anorg. Allg. Chem.* **1974**, *403*, 310. (d) Gysling, H. J. *Inorg. Synth.* **1979**, *19*, 96.

H_2O (5 cm^3) was added dropwise to form the yellow, crystalline product, yield 0.85 g (54%). The Ph_4As^+ salt can be similarly prepared as its hemihydrate.

Bis(tetraethylammonium) Cyano(oxotrithiotungstenio-*S*,*S*′)-cuprate(2−), $(Et_4N)_2[(CN)CuS_2WOS]$. Solid $K_3[WOS_3]Cl$[21c] (5.0 g, 11.1 mmol) was added to a stirred mixture of CuCN (1.0 g, 11.2 mmol) and KCN (1.0 g, 15.4 mmol) in H_2O (20 cm^3). After filtration, a solution of Et_4NBr (4.7 g, 22.4 mmol) in H_2O (10 cm^3) was added to form a pale yellow, crystalline precipitate. After the mixture was stirred for 5 min, the precipitate was filtered off, washed with 80% EtOH and then 95% EtOH, and dried under vacuum; yield 2.5 g (29%).

The cyano species described above are useful starting materials for the preparation of other species in high yields:

(a) A solution of $(n\text{-}Pr_4N)_2[(CN)CuS_2MoS_2]$ (0.75 g, 1.1 mmol) in MeCN (5 cm^3) was added to a stirred solution of $[(PPh_3)_2Cu(NO_3)]$[21d] (0.71 g, 1.1 mmol) in MeCN (10 cm^3). The red precipitate of $[(Ph_3P)_2CuS_2MoS_2Cu(PPh_3)]$[8a] was filtered off, washed with EtOH, acetone, and ether, and dried in the air; yield 0.6 g (72%, based upon available PPh_3).

(b) A solution of $(n\text{-}Pr_4N)_2[(CN)AgS_2WS_2]$ (0.2 g, 0.25 mmol) in MeCN (5 cm^3) was added to $[(PPh_3)_2Cu(NO_3)]$ (0.16 g, 0.25 mmol) in MeCN (20 cm^3). The yellow solution was stirred for 15 min, and the resulting yellow precipitate of $(PPh_3)_3CuAgWS_4$ was filtered off, washed with MeCN and ether, and dried in the air; yield 0.14 g (65%, based upon available PPh_3).

Nuclear Magnetic Resonance. ^{95}Mo and ^{183}W NMR spectra were obtained on a JEOL FX-200 spectrometer at operating frequencies of 13.00 and 8.31 MHz, respectively. Experimental conditions for ^{95}Mo NMR measurement have been described previously.[22] The ^{95}Mo chemical shifts are referenced to a solution of Na_2MoO_4 (2 M in ^2H_2O, apparent pH 11). For the ^{183}W measurements the magnetic field was locked and shimmed on the ^2H resonance of ^2H_2O in a solution of Na_2WO_4 (2 M) in a 15-mm spinning tube. Chemical shifts were referenced externally by using the sample replacement method. The sample has $\Xi = 4\,166\,388$ Hz. Chemical shifts (ppm) are calculated with positive values arising from resonances occurring at higher frequency than the reference solution. When nondeuterated solvents were used, field locking was achieved by locking onto the ^2H frequency of a ^2H_2O sample contained in an insert in the sample tube. All ^{183}W measurements were made at 20 °C. Sample concentration was 0.5–1.0 M where possible, generally 16 384 data points were used for spectral band widths of 5–20 kHz, and pulse repetition times were between 1 and 2 s.

X-ray Crystallography. Crystal data for compounds I–III are collected in Table I. Suitable crystals were mounted on glass fibers and lightly coated with epoxy resin: I, red-orange needles, 0.28 × 0.18 × 0.15 mm; II, red-orange chunky needles and plates frequently exhibiting twinning, sample—carefully cleaved fragment, 0.33 × 0.22 × 0.13 mm; III, yellow needles and plates, 0.24 × 0.12 × 0.16 mm. Precession photography indicated a triclinic space group in each case.

Lattice parameters (at 21 °C (I, III) and 26 °C (II)) were determined by a least-squares fit to the setting parameters of 25 independent reflections measured and refined by scans performed on an Enraf-Nonius CAD4 four-circle diffractometer.

Intensity data ($\pm h,\pm k,l$) were collected in the range $1.5 < \theta < x°$ (x = 27 (I), 25 (II, III)) by using ω–$(n/3)\theta$ scan where n, optimized by peak analysis, was 4 (I, III) or 5 (II). The ω scan angles and horizontal counter apertures employed were $(1.00 + 0.35 \tan \theta)°$ and $(2.40 + 0.5 \tan \theta)$ mm, respectively. Data reduction was performed by application of the program SUSCAD,[23] which also applied Lorentz and polarization corrections, while absorption corrections were applied by using the program ABSORB.[24]

The structures were solved by Patterson and Fourier techniques. The positions of heavier atoms (I, Mo, Cu; II, Mo, Cu, As; III, W) were located by direct methods using the SHELX[25] or MULTAN[26] systems of programs. Calculation of a difference map, with these atoms included, enabled the location of all other non-hydrogen atoms to be determined. For I and III, the aliphatic hydrogen atoms were included by assuming tetrahedral geometry (C–H = 0.97 Å). Only group temperature factors were refined. Similarly, for II, phenyl moieties were included and refined with group temperature factors as rigid planar groups (C–C = 1.395 Å) with associated hydrogen atoms (C–H = 0.95 Å). The water molecule is disordered over two sites, about 0.6 Å apart, with occupancies of 0.67 (7) and 0.33 (7). The associated hydrogen atoms were not located or included.

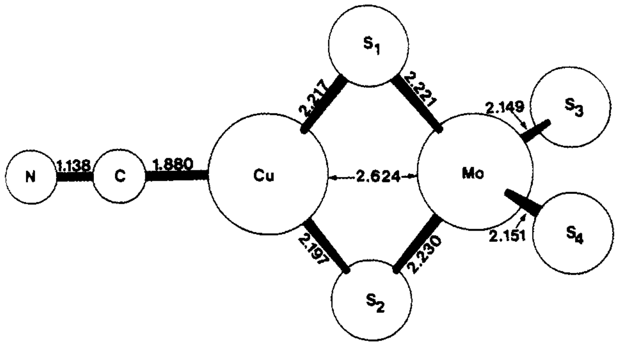

Figure 1. Structure of the anion in $(n\text{-}Pr_4N)_2[(CN)CuS_2MoS_2]$ (I) (PLUTO plot) and the atomic numbering scheme employed.

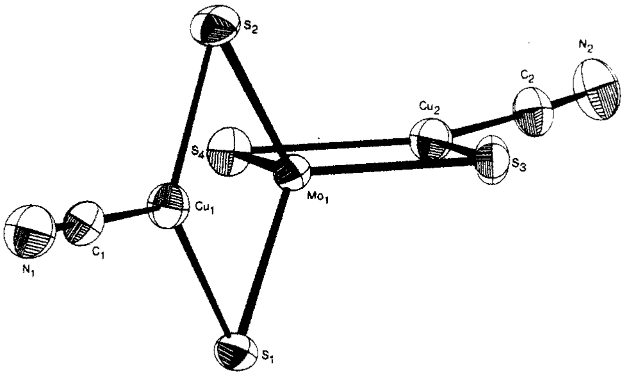

Figure 2. Structure of the anion in $(Ph_4As)_2[(CN)CuS_2MoS_2Cu(CN)]\cdot H_2O$ (II) (ORTEP plot) and the atomic numbering scheme employed.

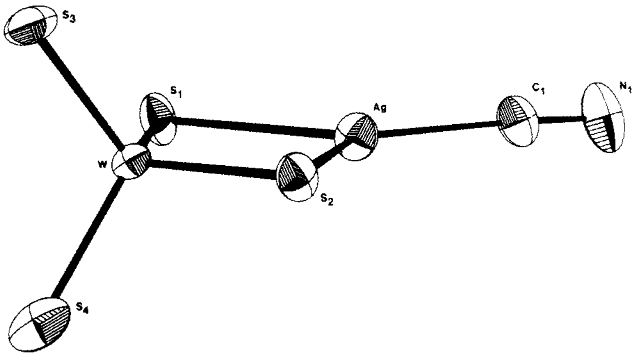

Figure 3. Structure of the anion in $(n\text{-}Pr_4N)_2[(CN)AgS_2WS_2]$ (III) (ORTEP plot) and the atomic numbering scheme employed.

With the exceptions listed above, all non-hydrogen atoms were refined anisotropically. Blocked- (I, III) or full- (II) matrix least-squares techniques were used to refine all positional and thermal parameters and an overall scale factor. A weighting scheme was applied and refined in each case, converging at $w = y/(\sigma^2 F_o + zF_o^2)$ (I, y = 4.3384, z = 0.0001; II, y = 2.23, z = 0.00063; III, y = 1.0, z = 0.0026). Overall refinement converged (all shifts less than 0.5σ (I, II), or 1.0σ (III)) with the final R and R_w factors listed in Table I. For I and III, a final difference map revealed a number of peaks of magnitude less than 1.5 e $Å^{-3}$ located in the vicinity of the Mo or W atom. For II, a number of peaks of magnitude less than 1 e $Å^{-3}$ remained. All were located in the phenyl groups along the carbon–carbon bonds and presumably arise because of the constraints applied.

---

(22) Gheller, S. F.; Hambley, T. W.; Brownlee, R. T. C.; O'Connor, M. J.; Snow, M. R.; Wedd, A. G. *J. Am. Chem. Soc.* **1983**, *105*, 1527.

(23) "SUSCAD, Data Reduction Program for the CAD4 Diffractometer"; University of Sydney, 1976.

(24) "ABSORB, Absorption Correction Program for the CAD4 Diffractometer"; University of Sydney, 1976.

(25) Sheldrick, G. M. "SHELX-76, Program for Crystal Structure Determination"; University of Cambridge, 1976.

(26) MULTAN: Germain, G.; Main, P.; Woolfson, M. M. *Acta Crystallogr., Sect. A* **1971**, *A27*, 368.

Table I. Crystallographic Data[a]

	$(n\text{-}Pr_4N)_2$-$[(CN)CuS_2MoS_2]$ (I)	$(Ph_4As)_2$-$[(CN)CuS_2MoS_2Cu(CN)]\cdot H_2O$ (II)	$(n\text{-}Pr_4N)_2$-$[(CN)AgS_2WS_2]$ (III)
formula	$C_{25}H_{56}CuMoN_3S_4$	$C_{50}H_{42}As_2Cu_2MoN_2OS_4$	$C_{25}H_{56}AgN_3S_4W$
mol wt	686.5	1188.0	818.7
a, Å	9.712 (1)	9.561 (2)	9.546 (3)
b, Å	12.686 (3)	15.158 (3)	13.009 (2)
c, Å	14.474 (2)	18.027 (2)	14.692 (2)
α, deg	76.07 (1)	97.45 (1)	75.62 (1)
β, deg	83.98 (1)	101.30 (1)	84.93 (2)
γ, deg	81.19 (1)	91.81 (2)	80.57 (2)
D_{measd}, g cm^{-3}	1.33	1.56 (2)	1.56 (2)
D_{calcd}, g cm^{-3}	1.299	1.556	1.561
V, Å	1705.96	2535.9	1741.3
μ(Mo Kα), cm^{-1}	12.10	25.31	41.50
F(000), electrons	721	1181	824
no. of reflcns measd	5108	9576	5596
no. of reflcns used ($I/\sigma(I) > 2.5$)	3709	4936	3957
R[b]	0.040	0.048	0.042
R_w[c]	0.046	0.054	0.044

[a] Triclinic space group $P\bar{1}$; $Z = 2$; λ(Mo Kα) = 0.7107 Å. [b] $R = \Sigma(|F_o| - |F_c|)/\Sigma|F_o|$. [c] $R_w = \Sigma(|F_o| - |F_c|)w^{1/2}/\Sigma(|F_o|w^{1/2})$.

Atomic coordinates and bond lengths and bond angles for the anions are given in Tables II and III, respectively. The molecular structures of the anions are shown in Figures 1–3, together with the atomic numbering schemes. Listings of observed and calculated structure factors and anisotropic thermal parameters for the non-hydrogen atoms, of the atomic coordinates, bond distances, and bond angles of the cations, and of the atomic coordinates and thermal parameters for the hydrogen atoms are included in Tables S1–S15 of the supplementary material.

Results and Discussion

Synthesis. The polymer $(NH_4)CuMoS_4$[21a,27] is cleaved by aqueous cyanide. Addition of quaternary cations allows the convenient isolation of the binuclear anion $[(CN)CuS_2MoS_2]^{2-}$ and, in the presence of 1 equiv of CuCN, the trinuclear anion $[(CN)CuS_2MoS_2Cu(CN)]^{2-}$:

$$[CuMoS_4]_n^{n-} + CN^- \rightarrow [(CN)CuS_2MoS_2]^{2-} \xrightarrow{Cu(CN)} [(CN)CuS_2MoS_2Cu(CN)]^{2-}$$

More generally, the addition of the $[MS_4]^{2-}$ (M = Mo, W) anions to $[M'(CN)_x]^{1-x}$ (M′ = Cu, Ag) systems in 1:1 proportions leads to the binuclear anions $[(CN)M'S_2MS_2]^{2-}$. If 1:2 proportions are used, the trinuclear anions $[(CN)M'S_2MS_2M'(CN)]^{2-}$ are produced, although only the species $[(CN)CuS_2MS_2Cu(CN)]^{2-}$ were isolated in high purity in the present work.

Similar procedures involving $[MOS_3]^{2-}$ and $[Cu(CN)_x]^{1-x}$ lead to $[(CN)CuS_2MOS]^{2-}$. The same products are precipitated when $[MO_2S_2]^{2-}$ replaces $[MOS_3]^{2-}$, but slow precipitation and moderate yields suggest the presence of complex equilibria in solution. Attempts to prepare the silver analogues were unsuccessful.

The cyano ligands are easily displaced in these anions. They are consequently useful starting materials for synthesis of related species:

$$[(CN)CuS_2MoS_2]^{2-} + PhS^- \rightarrow [(PhS)CuS_2MoS_2]^{2-}\ {}^{14}$$

$$[(CN)CuS_2MoS_2Cu(CN)]^{2-} + 2PhS^- \rightarrow [(PhS)CuS_2MoS_2Cu(SPh)]^{2-}\ {}^{14}$$

$$[(CN)CuS_2MS_2]^{2-} + [(PPh_3)_2Cu(NO_3)] \rightarrow [(PPh_3)_2CuS_2MS_2Cu(PPh_3)]\ {}^{8}$$

$$[(CN)AgS_2WS_4]^{2-} + [(PPh_3)_2Cu(NO_3)] \rightarrow (PPh_3)_3CuAgWS_4$$

Table II. Atomic Coordinates[a,b] (×10⁴) of Anions in I–III

compd	atom	x	y	z
I	Mo(1)	7770.4 (4)	3400.4 (3)	2732.4 (3)
	Cu(1)	7216.9 (7)	1673.4 (5)	2214.6 (5)
	S(1)	7295 (2)	1833 (1)	3700 (1)
	S(2)	7683 (2)	3218 (1)	1246 (1)
	S(3)	6237 (2)	4725 (1)	3002 (1)
	S(4)	9827 (1)	3696 (1)	2937 (1)
	C(1)	6832 (6)	425 (4)	1855 (4)
	N(1)	6613 (6)	−332 (4)	1633 (4)
II	Mo(1)	−365 (1)	2569 (1)	7645 (1)
	Cu(1)	−1085 (1)	848 (1)	7400 (1)
	S(1)	−651 (3)	1721 (1)	8519 (1)
	S(2)	−660 (3)	1689 (1)	6540 (1)
	C(1)	−1629 (10)	−381 (6)	7184 (5)
	N(1)	−1959 (11)	−1120 (5)	7043 (5)
	Cu(2)	147 (1)	4310 (1)	7871 (1)
	S(3)	−1973 (2)	3576 (1)	7583 (1)
	S(4)	1769 (2)	3290 (1)	7929 (1)
	C(2)	451 (8)	5559 (6)	7999 (5)
	N(2)	601 (9)	6314 (5)	8049 (5)
	O(1)[c]	607 (33)	2741 (8)	3263 (11)
	O(1′)[c]	9983 (69)	2676 (18)	3095 (23)
III	W(1)	2193	1516	2249
	Ag(1)	2799 (1)	3369	2809
	S(1)	2620 (3)	3032 (2)	1237 (2)
	S(2)	2221 (3)	1612 (2)	3739 (1)
	S(3)	137 (3)	1188 (2)	2006 (2)
	S(4)	3780 (3)	207 (2)	2018 (2)
	C(1)	3272 (11)	4711 (8)	3199 (6)
	N(1)	3570 (13)	5400 (8)	3412 (7)

[a] Estimated standard deviations in parentheses. [b] Anion atomic numbering schemes given in Figures 1–3. [c] The two oxygen sites associated with water of crystallization.

Microanalytical and infrared spectral data are provided in Table IV. The presence of coordinated cyanide is confirmed by the presence of strong, sharp absorptions in the range 2110–2147 cm^{-1} of the infrared[28a] spectrum. Two bands are observed in that range in certain salts that also contain lattice water, and the origin of the splitting appears to be due to hydrogen-bonding interactions between the coordinated cyanide and that lattice water. In $(Ph_4As)_2[(CN)CuS_2MoS_2Cu(CN)]\cdot H_2O$ (II), the water molecule is disordered over two sites, about 0.6 Å apart, which are both within hydrogen-bonding distance of the terminal nitrogens (Tables

---

(27) Binnie, W. P.; Redman, M. J.; Mallio, W. J. *Inorg. Chem.* **1970**, *9*, 1449.

(28) (a) Nakamoto, K. "Infrared and Raman Spectra of Inorganic and Coordination Compounds", 3rd ed.; Wiley: New York, 1978; p 259. (b) Schmidt, K. H.; Müller, A. *Coord. Chem. Rev.* **1974**, *14*, 115.

Table III. Bond Lengths (Å) and Angles (deg) for the Anions in I-III[a,b]

Compound I							
Mo(1)···Cu(1)	2.624 (1)			S(1)-Mo(1)-S(2)	106.7 (1)	S(1)-Mo(1)-S(3)	110.0 (1)
Mo(1)-S(1)	2.221 (1)	Mo(1)-S(2)	2.230 (2)	S(1)-Mo(1)-S(4)	109.9 (1)	S(2)-Mo(1)-S(3)	109.9 (1)
Mo(1)-S(3)	2.149 (2)	Mo(1)-S(4)	2.151 (2)	S(2)-Mo(1)-S(4)	109.9 (1)	S(3)-Mo(1)-S(4)	110.4 (1)
Cu(1)-S(1)	2.217 (2)	Cu(1)-S(2)	2.197 (1)	S(1)-Cu(1)-S(2)	108.1 (1)	Mo(1)-Cu(1)-C(1)	179.3 (2)
Cu(1)-C(1)	1.880 (6)	C(1)-N(1)	1.138 (9)	S(1)-Cu(1)-C(1)	125.7 (2)	S(2)-Cu(1)-C(1)	126.3 (2)
N(1)-C(1)	1.525 (6)			Mo-S(1)-Cu(1)	72.5 (1)	Mo(1)-S(2)-Cu(1)	72.7 (1)
				Cu(1)-C(1)-N(1)	179.3 (5)		
Compound II							
Mo(1)···Cu(1)	2.635 (1)	Mo(1)···Cu(2)	2.634 (1)	S(1)-Mo(1)-S(2)	107.3 (1)	S(1)-Mo(1)-S(3)	109.6 (1)
Mo(1)-S(1)	2.208 (2)	Mo(1)-S(2)	2.213 (2)	S(1)-Mo(1)-S(4)	111.6 (1)	S(2)-Mo(1)-S(3)	110.0 (1)
Mo(1)-S(3)	2.198 (2)	Mo(1)-S(4)	2.219 (2)	S(2)-Mo(1)-S(4)	111.0 (1)	S(3)-Mo(1)-S(4)	107.4 (1)
Cu(1)-S(1)	2.221 (3)	Cu(1)-S(2)	2.219 (2)	S(1)-Cu(1)-S(2)	106.6 (1)	S(3)-Cu(2)-S(4)	106.6 (1)
Cu(2)-S(3)	2.216 (2)	Cu(2)-S(4)	2.222 (2)	S(1)-Cu(1)-C(1)	128.9 (3)	S(2)-Cu(1)-C(1)	124.5 (3)
Cu(1)-C(1)	1.888 (9)	Cu(2)-C(2)	1.884 (9)	S(3)-Cu(2)-C(2)	125.1 (2)	S(4)-Cu(2)-C(2)	128.2 (2)
C(1)-N(1)	1.137 (10)	C(2)-N(2)	1.138 (10)	Mo-S(1)-Cu(1)	73.0 (1)	Mo(1)-S(2)-Cu(1)	73.0 (1)
N(1)···O[c]	2.853 (25)	N(2)···O[c]	2.982 (23)	MoS(3)-Cu(2)	73.2 (1)	Mo(1)-S(4)-Cu(2)	72.7 (1)
N(1)···O′ [c]	3.083 (34)	N(2)···O′ [c]	2.708 (31)	Cu(1)-C(1)-N(1)	179.1 (9)	Cu(2)-C(2)-N(2)	177.4 (8)
Compound III							
W(1)···Ag(1)	2.890 (1)	W(1)-S(2)	2.225 (2)	S(1)-W(1)-S(2)	112.3 (1)	S(1)-W(1)-S(3)	108.8 (1)
W(1)-S(1)	2.229 (2)	W(1)-S(4)	2.158 (3)	S(1)-W(1)-S(4)	109.5 (1)	S(2)-W(1)-S(3)	108.9 (1)
W(1)-S(3)	2.153 (3)	Ag(1)-S(2)	2.476 (2)	S(2)-W(1)-S(4)	108.6 (1)	S(3)-W(1)-S(4)	108.6 (1)
Ag(1)-S(1)	2.481 (3)	C(1)-N(1)	1.105 (16)	S(1)-Ag(1)-S(2)	96.5 (1)	W(1)-Ag(1)-C(1)	179.0 (3)
Ag(1)-C(1)	2.093 (11)			S(1)-Ag(1)-C(1)	131.1 (2)	S(2)-Ag(1)-C(1)	132.4 (2)
				W(1)-S(1)-Ag(1)	75.5 (1)	W(1)-S(2)-Ag(1)	75.6 (1)
				Ag(1)-C(1)-N(1)	177.4 (9)		

[a] Estimated standard deviations in parentheses. [b] Anion atomic numbering schemes given in Figures 1-3. [c] O and O′ represent the two sites for the water of crystallization.

Table IV. Characterization Data

	microanalysis,[a] %				IR maxima,[g] cm^{-1}			
compd	C	H	N	S	ν(CN)	ν(MS)	ν(MO)	ν(OH)
$(n\text{-Pr}_4N)_2[(CN)CuS_2MoS_2]$[b]	43.62 (43.76)	8.45 (8.22)	5.92 (6.12)	17.90 (18.68)	2120	500, 489, 452, 410		
$(n\text{-Pr}_4N)_2[(CN)AgS_2MoS_2]$	40.91 (41.09)	7.54 (7.72)	5.65 (5.75)	17.66 (17.55)	2127	500, 494, 449, 436, 352		
$(n\text{-Pr}_4N)_2[(CN)CuS_2WS_2]$	38.71 (38.78)	7.11 (7.29)	5.34 (5.43)	16.46 (16.56)	2120	490, 482, 450 sh, 444, 415		
$(n\text{-Pr}_4N)_2[(CN)AgS_2WS_2]$	36.81 (36.68)	6.76 (6.89)	5.15 (5.13)	15.85 (15.67)	2138	498, 486, 441, 358		
$(Et_4N)_2[(CN)CuS_2MoS_2Cu(CN)]\cdot H_2O$	31.90 (31.71)	6.04 (6.21)	8.37 (8.22)	18.82 (18.81)	2142	475, 434		3500, 3430, 1650, 630
$(Ph_4As)_2[(CN)CuS_2McS_2Cu(CN)]\cdot H_2O$[c]	50.53 (50.55)	3.66 (3.56)	2.21 (2.36)	10.67 (10.80)	2140	428		
$(n\text{-Pr}_4N)_2[(CN)CuS_2MoS_2Cu(CN)]\cdot H_2O$	39.40 (39.33)	7.25 (7.36)	6.95 (7.06)	16.32 (16.15)	2142, 2132	480, 432		3570, 3440, 1648, 640
$(n\text{-Pr}_4N)_2[(CN)CuS_2WS_2Cu(CN)]\cdot H_2O$	35.38 (35.41)	6.59 (6.63)	6.27 (6.35)	14.67 (14.54)	2147, 2140	470, 435		3570, 3440, 1652, 625
$(Ph_4As)_2[(CN)CuS_2MoOS]\cdot 0.5H_2O$[d]	54.66 (54.83)	3.72 (3.85)		8.89 (8.96)	2123, 2114	495, 458	888	3500, 3460, 1620
$(Et_4N)_2[(CN)CuS_2MoOS]$[e]	36.76 (36.58)	7.11 (7.22)	7.58 (7.53)	17.30 (17.23)	2140	499, 462, 424, 326	893	
$(Et_4N)_2[(CN)CuS_2WOS]$[f]	31.57 (31.60)			14.97 (14.89)	2110	473, 439, 413, 314	900	

[a] Calculated in parentheses. [b] Cu, 9.30 (9.26). [c] As, 12.35 (12.61). [d] O, 2.12 (2.24). [e] O, 2.99 (2.87). [f] O, 2.65 (2.48). [g] KBr disks.

II and III). In addition, exposure of the hydrated salts to vacuum (or, indeed, to the heat generated by the beam of the infrared spectrometer) leads to a single absorption in the ν(CN) range.

Two bands attributable to the ν(MS) stretching modes of e and b_2 symmetry are observed in the 400–500-cm^{-1} range[28b] for the anions $[(CN)CuS_2MS_2Cu(CN)]^{2-}$, consistent with D_{2d} point symmetry. However, more than the expected four maxima (2a,b_1 and b_2 modes in C_{2v} symmetry) are seen for some of the $[(CN)M'S_2MS_2]^{2-}$ salts. More definitive information must await detailed infrared, Raman, and resonance Raman studies that are presently in progress.

The presence of strong absorptions in the range 880–900 cm^{-1} for the salts $A_2[(CN)CuS_2MOS]$ indicates the presence of terminal oxo ligands in these species.

Structures[29] of $(n\text{-Pr}_4N)_2[(CN)M'S_2MS_2]$ (I, M = Mo, M′ = Cu; III, M = W, M′ = Ag). A summary of important dimensions of I and III is given in Table V, together with equivalent data, where available, for related species with anionic peripheral ligands (CN^-, SPh^-).

The M–S_t and M–S_b distances in I and II are similar, consistent with the similar ionic radii of Mo(VI) and W(VI).[31] The Ag–S_b distance of 2.478 (5) Å is significantly longer than

---

(29) Crystals of $(n\text{-Pr}_4N)_2[(CN)AgS_2MoS_2]$ (cell data: a = 9.534 (3), b = 13.016 (3), c = 14.709 (4) Å; α = 75.67 (2), β = 85.06 (2), γ = 80.71 (2)°; V = 1743.34 Å^3) are isostructural with I and III, but the structure was not solved as that of the $[Ph_4P]^+$ salt is now available.[30,8b]

(30) Müller, A., personal communication.

(31) (a) Shannon, R. D.; Prewitt, C. T. *Acta Crystallogr., Sect. B* **1970**, *B26*, 1076. (b) Shannon, R. D. *Acta Crystallogr., Sect. A* **1976**, *A32*, 751.

Table V. Comparative Structural Parameters[a]

compd	M--M′	M-S_t	M-S_b	M′-S_b	S_bMS_b	$S_bM'S_b$	MS_bM'	S_bMS_t	S_tMS_t	ref
$(n\text{-}Pr_4N)_2[(CN)CuS_2MoS_2]$ (I)	2.624 (1)	2.150 (3)	2.225 (7)	2.217 (2) 2.197 (1)	106.7 (1)	108.1 (1)	72.6 (2)	109.9 (2)	110.4 (1)	this work
$(Ph_4P)_2[(CN)CuS_2MoS_2]$	2.630 (1)	2.163 (2)	2.245 (2)	2.215 (2)						13
$(Ph_4P)_2[(CN)AgS_2MoS_2]$	2.868 (1)	2.160 (4)	2.212 (2) 2.223 (3)	2.506 (3) 2.475 (3)						6, 8[b]
$(n\text{-}Pr_4N)_2[(CN)AgS_2WS_2]$ (III)	2.890 (1)	2.155 (6)	2.227 (4)	2.478 (5)	112.3 (1)	96.5 (1)	75.5 (2)	109.0 (5)	108.6 (1)	this work
$(Ph_4As)_2[(CN)CuS_2MoS_2Cu(CN)]\cdot H_2O$ (II)	2.635 (1)		2.208 (2) 2.213 (2) 2.198 (2) 2.219 (2)	2.220 (6)	107.4 (2)[c] 110.6 (1.1)[d]	106.6 (1)	73.0 (4)			this work
$(Me_4N)_2Cu_2(CN)_2MoS_4$			2.209 (3)	2.300 (4)						13
$(n\text{-}Pr_4N)_2[(PhS)CuS_2MoS_2]$	2.636 (1)	2.166 (2) 2.157 (2)	2.227 (2) 2.214 (2)	2.198 (2) 2.224 (2)	106.7 (1)	107.3 (1)	73.0 (2)	111.1 (1) 109.6 (1) 109.8 (1) 108.3 (1)	111.2 (1)	14
$(n\text{-}Pr_4N)_2[(PhS)CuS_2MoS_2Cu(SPh)]$	2.632 (1)		2.210 (2) 2.201 (2)	2.212 (3)	106.7 (1)	107.3 (1)	73.0 (2)			14
$(NH_4)CuMoS_4$	2.70		2.19 (3)	2.31 (3)	110 (1)	102 (1)[e] 113 (1)[f]				27
$(NH_4)_2[MoS_4]$		2.17 (4)								*g*
$(NH_4)_2[WS_4]$		2.165 (11)								*h*

[a] Bond distances in Å, bond angles in degrees. [b] Müller, A., personal communication. [c] S_1MoS_2 of Figure 2. [d] S_1MoS_3 of Figure 2. [e] Two equivalent angles. [f] Four equivalent angles. [g] Schäfer, H.; Schäfer, G.; Weiss, A. *Z. Naturforsch., B: Anorg. Chem., Org. Chem., Biochem., Biophys. Biol.* **1964**, *19B*, 76. [h] Sasari, K. *Acta Crystallogr.* **1963**, *16*, 719.

the Cu–S_b distances of 2.217 (2) and 2.197 (1) Å. The difference, ca. 0.27 Å, is in the range 0.18–0.31 Å estimated[32] for the difference in the ionic radii of Cu(I) and Ag(I). The variation in bond angles within the $Cu(S_b)_2Mo$ and $Ag(S_b)_2W$ planes is striking. In particular, the $S_bM'S_b$ angle decreases dramatically from 108.1 (1) to 96.5 (1)°, the S_bMS_b angle increases from 106.7 (1) to 112.3 (1)°, and the MS_bM' angles alter from 72.6 (2) to 75.5 (2)°. The observations can be rationalized by the need to accommodate the larger Ag atom, coupled with a requirement for an acute MS_bM' angle of 72–79°. The latter range is observed[2] for related species of the type $[M'(MS_4)_2]^{2-}$ (M′ = Zn, Ni, Co), $[X_2FeS_2MoS_2]^{2-}$ (X = Cl, SPh), $[Cl_2FeS_2MoS_2FeCl_2]^{2-}$, $[(Ph_2MeP)AuS_2WS_2Au(PPh_2Me)]$, and $[(Ph_3P)_2AgS_2WS_2Ag(PPh_3)]$ and may be partly related to the spatial requirements of the two "lone pairs" on S_b. In addition, the observed S_bMS_b angles in such compounds are in the range 102–113°. It appears, therefore, that in III both the MS_bM' and S_bMS_b angles open out to accommodate the larger Ag atom, and the longer Ag–S_b bond then dictates a smaller $S_bM'S_b$ bond angle, which is acceptable to the stereochemically flexible Ag("d^{10}") atom.

The $Cu(S_b)_2Mo$ and $Ag(S_b)_2W$ moieties of I and III are planar to within 0.002 and 0.01 Å, respectively.[33] The intermetal M′---M distances are similar for $[(CN)AgS_2MS_2]^{2-}$ (M = Mo, W) and increased by 0.24–0.28 Å over that for $[(CN)CuS_2MoS_2]^{2-}$, again in keeping with the larger ionic radius of Ag(I). However, these distances are only slightly greater (ca. 0.1 Å) than the sum of reasonable estimates of the atomic radii of M and M′ in these environments, and significant MM′ bonding (M′(I) (d^{10}) → M(VI) (d^0) charge delocalization) is a possibility. Certainly, compounds containing MS_4 ligands bound to *open-shell* metals M′ show[2] properties characteristic of strongly delocalized molecular orbitals. However, as observed previously for the $[(PhS)CuS_2MoS_2]^{2-}$ anion,[14] supporting spectroscopic evidence for the present anions is lacking.

Structure of $(Ph_4As)_2[(CN)CuS_2MoS_2Cu(CN)]\cdot H_2O$ (II). The crystal structure consists of discrete complex anions (Figure 2), Ph_4As cations, and a disordered water molecule. The only close contacts are between the terminal nitrogens of the CN ligands and each of the sites of the water molecule (Table III).

The molecular structure of the $[(CN)CuS_2MoS_2Cu(CN)]^{2-}$ anion is closely related to that of $[(CN)CuS_2MoS_2]^{2-}$ and of $[(PhS)CuS_2MoS_2Cu(SPh)]^{2-}$[14] (Table V). The slight changes in bond lengths and angles are those expected when a second CuCN fragment binds to the terminal sulfur ligands of $[(CN)CuS_2MoS_2]^{2-}$. However, the anion is somewhat distorted from maximum symmetry, D_{2d}, by bends in the NC–Cu–Mo–Cu–CN axis at all three metal atoms. Thus, the Cu(1)–Mo–Cu(2) angle is 175.7 (1)°, and the S_b–Cu–C bond angles about each copper are not equal (Table III). Interestingly, however, similar distortions are observed about each copper atom and presumably arise from the hydrogen-bonding or crystal-packing interactions.

The crystal structure is very different from that[13] of another salt of similar stoichiometry, $(Me_4N)_2Cu_2(CN)_2MoS_4$, which may be described as a zigzag...CuCNCuCNCu...chain with the binuclear anion $[(CN)CuS_2MoS_2]^{2-}$ bound as a bidentate ligand to each of the copper atoms of the chain. Consequently, the chain copper atoms are in a distorted-tetrahedral site. It is probable that the larger cation in the Ph_4As^+ salt described

---

(32) Cotton, F. A.; Wilkinson, G. "Advanced Inorganic Chemistry", 4th ed.; Wiley: New York, 1980; p 14.

(33) The least-squares plane through CuS(1)S(2)Mo in I is $0.9746x - 0.2237y - 0.0099z = 6.0245$ [atom deviations (Å): Mo, −0.0022; Cu, −0.0024; S(1), 0.0023; S(2), 0.0023]. The equivalent plane through AgS(1)S(2)W in III is $0.9744x - 0.2245y - 0.0099z = 1.4561$ [atom deviations (Å): W, 0.0155, Ag, 0.0117; S(1), −0.0136; S(2), −0.0137].

Table VI. Electronic Spectra in DMF

compd	λ,[a] nm ($10^{-3}\epsilon$, M^{-1} cm^{-1})
$(Et_4N)_2[MoS_4]$	477 (14.25), 324 (20.60)
$(n\text{-}Pr_4N)_2[(CN)CuS_2MoS_2]$	471 (6.19), 460 (sh), 319 (19.18)
$(n\text{-}Pr_4N)_2$-$[(CN)CuS_2MoS_2Cu(CN)]\cdot H_2O$	492 (4.76), 456 (sh), 340 (sh), 314 (16.87)
$(Ph_4As)_2$-$[(CN)CuS_2MoS_2Cu(CN)]\cdot H_2O$	492 (4.88), 457 (sh), 340 (sh), 314 (17.40)
$(n\text{-}Pr_4N)_2[(CN)AgS_2MoS_2]$	469 (9.56), 317 (16.51)
$(Et_4N)_2[(CN)CuS_2MoOS]$	427 (3.42), 391 (4.14), 320 (sh), 296 (9.81)
$(NH_4)_2[WS_4]$	398 (17.08), 283 (24.81)
$(n\text{-}Pr_4N)_2[(CN)CuS_2WS_2]$	396 (9.63), 284 (23.95)
$(Pr_4N)_2$-$[(CN)CuS_2WS_2Cu(CN)]\cdot H_2O$	409 (7.14), 398 (sh), 291 (24.20)
$(n\text{-}Pr_4N)_2[(CN)AgS_2WS_2]$	392 (10.51), 284 (24.21)
$(Et_4N)_2[(CN)CuS_2WOS]$	366 (4.70), 338 (5.84), 280 (sh)

[a] sh, shoulder.

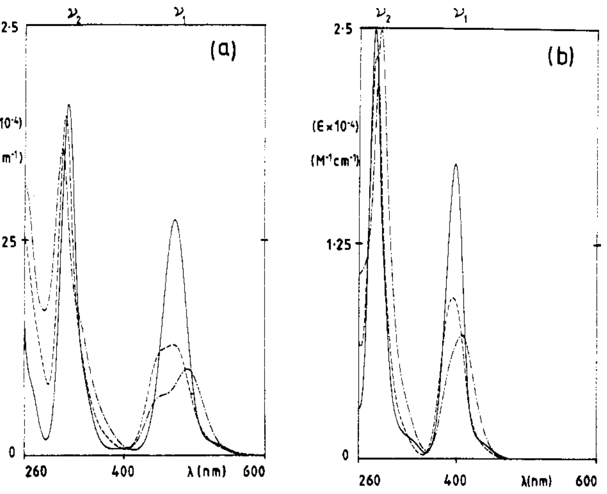

Figure 4. Electronic spectra: (a) $(Et_4N)_2[MoS_4]$ (—), $(n\text{-}Pr_4N)_2[(CN)CuS_2MoS_2]$ (---), and $(n\text{-}Pr_4N)_2[(CN)CuS_2MoS_2Cu(CN)]\cdot H_2O$ (–·–) in DMF; (b) $(NH_4)_2[WS_4]$ (—), $(n\text{-}Pr_4N)_2[(CN)CuS_2WS_2]$ (---), and $(n\text{-}Pr_4N)_2[(CN)CuS_2WS_2Cu(CN)]\cdot H_2O$ (–·–) in DMF.

in the present work destabilizes the chain structure relative to that containing the discrete trinuclear anion. However, the crystal structures of members of the series $A_2M'_2(CN)_2MS_4$ may show interesting variations with cation A, especially given the stereochemical flexibility of M′ and the bridging capability of the cyanide ligand. In the present work, the presence of a lattice H_2O in each of the salts $A_2Cu(CN)_2MS_4$ isolated in high purity (Table V) coupled with their similar infrared properties suggests the presence of discrete $[(CN)CuS_2MS_2Cu(CN)]^{2-}$ anions in each case. However, further structural characterization is needed.

Electronic Spectra. The spectra of the anions $[MS_4]^{2-}$, $[(CN)M'S_2MS_2]^{2-}$, $[(CN)CuS_2MS_2Cu(CN)]^{2-}$, and $[(CN)CuS_2MOS]^{2-}$ are listed in Table VI and shown in Figure 4.

A simple MO scheme for the $[MS_4]^{2-}$ ions may be devised[2] by assuming nd, $(n + 1)$s, and $(n + 1)$p valence orbitals on M and 3s and 3p valence orbitals on S. The longest wavelength absorptions at 477 and 398 nm for M = Mo and W, respectively, can be unambiguously assigned[2] to the one-electron transition ν_1:$t_1(n, \pi) \rightarrow 2e(d)$ on the basis of magnetic circular dichroism measurements. In addition, the absorptions at 324 and 283 nm for M = Mo and W, respectively, are plausibly assigned[2] to ν_2:$3t_2(\pi, \sigma) \rightarrow 2e(d)$.

From Figure 4, it can be seen that (i) the binuclear and trinuclear complexes absorb in the same energy regions as $[MS_4]^{2-}$, (ii) the spectra of the species $[(CN)M'S_2MS_2]^{2-}$ are essentially independent of M′ = Cu or Ag, (iii) absorption of the complexes in the ν_1 region is split typically into at least two bands, although in some cases individual inflection points are not resolved, and (iv) absorption of the complexes in the ν_2 region is essentially unaltered in position, intensity, and peak width from that of the $[MS_4]^{2-}$ ions.

Table VII. ^{95}Mo and ^{183}W Chemical Shift Data (ppm) for $[MO_{4-n}X_n]^{2-}$ (n = 0–4)

	M = Mo,[a] X = S		M = Mo,[a] X = Se		M = W,[b] X = S
anion	H_2O[c]	MeCN	H_2O[c]	MeCN	D_2O[d]
$[MO_4]^{2-}$	0	*e*	0	*e*	0
$[MO_3X]^{2-}$	497	*e*	656	*e*	841
$[MO_2X_2]^{2-}$	1066	964	1450	1335	1787
$[MOX_3]^{2-}$	1654	1587	2272	2171	2760
$[MX_4]^{2-}$	2258	2207	3145	3339	3769[f]

[a] [Mo] = 0.1 M; see text for cations employed; line widths <10 Hz. [b] [W] = 0.25–0.5 M; see text for cations employed; line widths <1 Hz. [c] pH 7–10. [d] pD 7–9. [e] Not observed. [f] 3659 ppm in DMF.

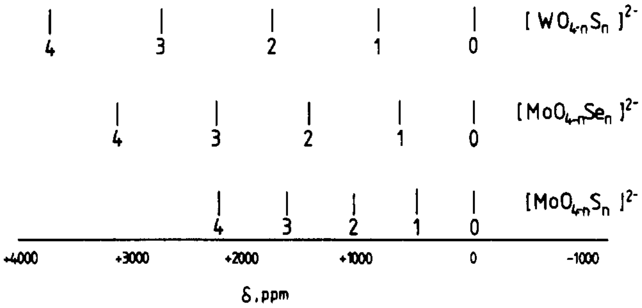

Figure 5. ^{95}Mo and ^{183}W chemical shift scale for $[MO_{4-n}X_n]^{2-}$, relative to aqueous 2 M $[MO_4]^{2-}$, pH 11.

It is apparent that the spectra of the complexes are dominated by the internal transitions of the $[MS_4]^{2-}$ ions. The splitting of the ν_1 absorption is plausibly due to the raising of the degeneracy of the $t_1(n, \pi)$ level in the lower symmetry of the complexes (t_1 (T_d) $\leftrightarrow$ a_2 + e (D_{2d}) $\leftrightarrow$ $a_2 + b_1 + b_2$ (C_{2v})). As the 2e(d) level appears to be involved in both ν_1 and ν_2, but ν_2 is essentially unaffected by complex formation, it is unlikely that the splitting of ν_1 is dominated by raising the degeneracy of 2e(d). Of course, the above rationalization ignores electron repulsion and spin–orbit coupling effects, and detailed work is needed for definitive answers. Müller[2] has drawn similar initial conclusions from comparison of the spectra of the two species $[MoS_4]^{2-}$ and $[(CN)CuS_2MoS_2]^{2-}$ in MeCN and further notes that a third intense absorption observed for $[MoS_4]^{2-}$ in the 240–280-nm range (which is assigned to originate in $t_1(n, \pi)$) is also split into at least three bands in $[(CN)CuS_2MoS_2]^{2-}$.

The anions $[MOS_3]^{2-}$ show[2] two intense low-energy absorptions (M = Mo, 465, 392 nm; M = W, 375, 334 nm). The species $[(CN)CuS_2MOS]^{2-}$ also exhibit two bands in those ranges (Table VI), and the spectra appear to be little influenced by coordination of the CuCN fragment.

^{95}Mo and ^{183}W Nuclear Magnetic Resonance. ^{95}Mo chemical shifts for the anions $[MoO_{4-n}X_n]^{2-}$ (X = S, Se; n = 0–4) in H_2O and MeCN as well as ^{183}W data for $[WO_{4-n}S_n]^{2-}$ in D_2O can be found in Table VII and are illustrated schematically in Figure 5. Aqueous solutions examined were obtained by dissolution of the salts $(NH_4)_2[MX_4]$, $K_3[MOS_3]Cl$, or $(NH_4)_2[MO_2X_2]$. Methyl cyanide solutions were prepared from these salts in the presence of 2 equiv of dried Et_4NCl. Resonances due to $[MOX_3]^{2-}$ were observed in both aqueous and MeCN solutions prepared from $(NH_4)_2[MX_4]$ and $(NH_4)_2[MO_2X_2]$. The peaks assigned to $[MoO_3X]^{2-}$ appeared in aqueous but not MeCN solutions of $(NH_4)_2[MoO_2X_2]$, while that of $[WO_3S]^{2-}$ was observed in an aqueous mixture

Table VIII. Solvent Dependence of the ^{95}Mo Chemical Shift of $(Et_4N)_2[MoS_4]$ (0.1 M)

solvent	δ	solvent	δ
H_2O	2252	MeCN	2207
D_2O	2251	DMF	2192
MeOH	2229	dmtf	2187
$MeNO_2$	2208	Me_2SO	2176

of $[WO_4]^{2-}$ and $[WO_2S_2]^{2-}$ in 4:1 molar proportion. The thermodynamic instability of the various metalates to sulfide and selenide exchange in solution and to further reaction mediated by protonation and redox steps is well established.[2,6] In the present work, $[MoOS_3]^{2-}$ was present in an MeCN solution of $(Et_4N)_2[MoO_2S_2]$ after 15 min, and after 5 days, the sample exhibited resonances due to $[MoOS_3]^{2-}$ and $[MoS_4]^{2-}$ only. However, resonances due to further reaction products such as $[Mo^V{}_2O_2(\mu\text{-}S)_2(S_2)_2]^{2-}$[34] were not observed, presumably due to low relative concentrations and/or broad line widths.[12]

The assignments of Table VII and Figure 5 are based upon the internal consistency of the results. The molybdenum anions exhibit uniformly narrow (<10 Hz) line widths and a similar solvent dependence of the chemical shift. A systematic decrease in shielding of the metal nuclei occurs with successive substitution of ligand O by S or Se. This downfield shift is respectively 497–604 ppm per S and 656–873 ppm per Se in $[MoO_{4-n}X_n]^{2-}$ in aqueous solution, while the corresponding range for $[WO_{4-n}S_n]^{2-}$ is 841–1009 ppm. The range observed[35] for $[MoO_{2-n}S_n(R_2NO)_2]$ (n = 0–2) in CH_2Cl_2 is 690–730 ppm. In addition, within these ranges, there is a consistent increase in the chemical shift difference between neighboring members of the series: e.g., 497, 569, 588, 604 for $[MoO_{4-n}S_n]^{2-}$ in H_2O.

The cation dependence of the chemical shift of $[MoS_4]^{2-}$ in the salts $A_2[MoS_4]$ (A = NH_4, K, Me_4N, Et_4N, Ph_4As (0.1 M)) is 2258–2252 ppm in H_2O and 2197–2188 ppm in DMF. Shielding increases slightly with increasing size of the cation, the opposite trend to that observed[16a] for $A[MoO_4]$ (A = Li, NH_4, Na, K (1.0 M)) in H_2O. In contrast, the solvent dependence of the chemical shift of $[MoS_4]^{2-}$ is pronounced, being over 70 ppm in the solvents examined (Table VIII). Correlations of chemical shift and solvent donor number[36a] have been reported[36b] for alkali metal nuclei and appear to reflect interaction between the basic solvents and the acidic metal cations. For $[MoS_4]^{2-}$, no correlation of ^{95}Mo chemical shift and solvent number could be discerned. The negative charge on $[MoS_4]^{2-}$ ensures that its solvation requirements are very different from those of (bare) alkali metal cations. The solvent dependence of the ^{59}Co resonance in $K_3[Co(CN)_6]$ shows a shift to higher field (the chemical shifts are more negative) in the order Me_2SO > MeCN >> MeOH > H_2O, a trend interpreted[37] as following the H-bond donor capabilities of the solvents. This qualitative order is *reversed* for $[MoS_4]^{2-}$ (Table VIII). An increase in coordination number promoted by protonation of ligand sulfide[6] by the protic solvents may be a further factor.

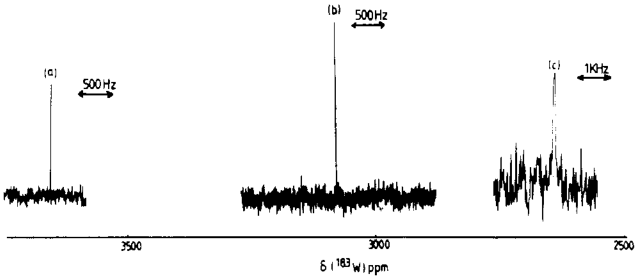

Figure 6. ^{138}W NMR in DMF at 20 °C: (a) 1 M $(NH_4)_2[WS_4]$ (3400 pulses; pulse repetition time 2.0 s; spectral width 10 kHz); (b) 0.5 M $(n\text{-}Pr_4N)_2[(CN)CuS_2WS_2]$ (20 000 pulses; pulse repetition time 1.0 s; spectral width 10 kHz); (c) 0.52 M $(n\text{-}Pr_4N)_2[(CN)CuS_2WS_2Cu(CN)]\cdot H_2O$ (82 000 pulses; pulse repetition time 1.0 s; spectral width 20 kHz).

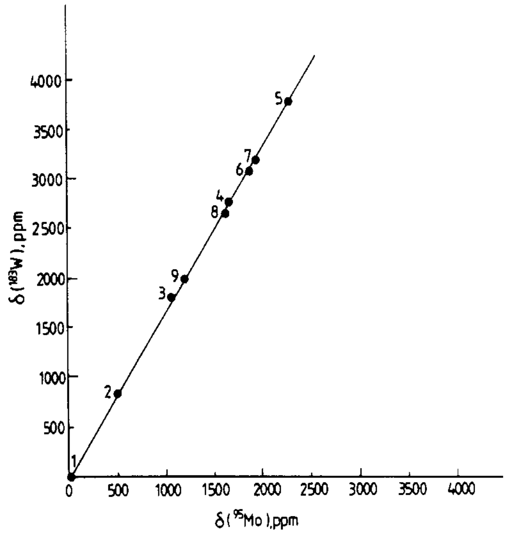

Figure 7. Plot of $\delta(^{183}W)$ vs. $\delta(^{95}Mo)$ (M = Mo, W): 1, $[MO_4]^{2-}$; 2, $[MO_3S]^{2-}$; 3, $[MO_2S_2]^{2-}$, 4, $[MOS_3]^{2-}$; 5, $[MS_4]^{2-}$; 6, $[(CN)CuS_2MS_2]^{2-}$; 7, $[(CN)AgS_2MS_2]^{2-}$; 8, $[(CN)CuS_2MS_2Cu(CN)]^{2-}$; 9, $[(CN)CuS_2MOS]^{2-}$.

^{95}Mo and ^{183}W chemical shifts for the binuclear anions $[(CN)M'S_2MS_2]^{2-}$ (M' = Cu, Ag; M = Mo, W) and $[(CN)CuS_2MOS]^{2-}$ (M = Mo, W) and the trinuclear anions $[(CN)CuS_2MS_2Cu(CN)]^{2-}$ (M = Mo, W) are given in Table IX, and representative ^{183}W spectra are shown in Figure 6. The resonances are all shielded with respect to the corresponding $[MS_4]^{2-}$ or $[MOS_3]^{2-}$ anions (Table VII). For example, cf. the following resonances (ppm). In MeCN: $[MoS_4]^{2-}$, 2207; $[(CN)CuS_2MoS_2]^{2-}$, 1863; $[(CN)CuS_2MoS_2Cu(CN)]^{2-}$, 1616. In dmf: $[WS_4]^{2-}$, 3659.0; $[(CN)CuS_2WS_2]^{2-}$, 3084.4; $[(CN)CuS_2WS_2Cu(CN)]^{2-}$, 2640.5. The CuCN moiety is more shielding than the AgCN moiety.

The most striking feature of the ^{183}W and ^{95}Mo chemical shifts for all the compounds examined in the present paper is their constant ratio, $\delta(W):\delta(Mo) = 1.67 \pm 0.03$, as clearly illustrated in Figure 7. This ratio can be compared with that of 1.7 observed[19,38,39] for an extensive series of low oxidation state species of the type $[M^0(CO)_5L]$, *cis*-$[M^0(CO)_4L_2]$ (L = phosphine, phosphite, piperidine), and $[M^{II}(CO)_3(\eta^5\text{-}C_5H_5)X]$ (X = Cl, Br, I).

Making the usual assumption that heavy-atom shielding is dominated by the paramagnetic term of the Ramsey equation,[40–42] the ratio of chemical shifts should be given by eq 1,

$$\frac{\delta(W)}{\delta(Mo)} = \frac{\Delta E(Mo)}{\Delta E(W)}\left[\frac{\langle r^{-3}\rangle_{6p\,W}P_i(W) + \langle r^{-3}\rangle_{5d\,W}D_i(W)}{\langle r^{-3}\rangle_{5p\,Mo}P_i(Mo) + \langle r^{-3}\rangle_{4d\,Mo}D_i(Mo)}\right] \quad (1)$$

---

[34] Rittner, W.; Müller, A.; Neumann, A.; Bäther, W.; Sharma, R. C. *Angew. Chem., Int. Ed. Engl.* **1979**, *18*, 530.

[35] Gheller, S. F.; Hambley, T. W.; Traill, P. R.; Brownlee, R. T. C.; O'Connor, M. J.; Snow, M. R.; Wedd, A. G. *Aust. J. Chem.* **1982**, *35*, 2183.

[36] (a) Gutman, V. *Coord. Chem. Rev.* **1976**, *18*, 225. (b) Dechter, J. J. *Prog. Inorg. Chem.* **1982**, *29*, 285.

[37] Eaton, D. R.; Rogerson, C. V.; Sandercock, A. C. *J. Phys. Chem.* **1982**, *86*, 1365.

[38] Le Gall, J.-Y.; Kubicki, M. M.; Petillon, F. Y. *J. Organomet. Chem.* **1981**, *221*, 287.

[39] McFarlane, H. C. E.; McFarlane, W.; Rycroft, D. S. *J. Chem. Soc., Dalton Trans.* **1976**, 1616.

Table IX. ^{95}Mo and ^{183}W NMR Data for Cyanide Complexes

compd	concn, M	solvent (T, °C)	δ	$W_{h/2}$, Hz
$(n\text{-Pr}_4\text{N})_2[(\text{CN})\text{CuS}_2\text{MoS}_2]$	0.1	MeCN	1863	38
		DMF	1854	93
$(n\text{-Pr}_4\text{N})_2[(\text{CN})\text{AgS}_2\text{MoS}_2]$	0.2	MeCN	1921	15
		DMF	1921	20
$(\text{Et}_4\text{N})_2[(\text{CN})\text{CuS}_2\text{MoS}_2\text{Cu}(\text{CN})]\cdot\text{H}_2\text{O}$	0.2	MeCN	1616	220
	0.6	DMF (20)	1606	900
		(52)	1610	300
		(80)	1612	210
		(100)	1616	140
$(\text{Et}_4\text{N})_2[(\text{CN})\text{CuS}_2\text{MoOS}]$	0.1	MeCN	1199	25
$(\text{Ph}_4\text{As})_2[(\text{CN})\text{CuS}_2\text{MoOS}]$	0.1	MeCN	1198	26
		DMF	1193	46
$(n\text{-Pr}_4\text{N})_2[(\text{CN})\text{CuS}_2\text{WS}_2]$	0.5	DMF	3084.4	*a*
$(n\text{-Pr}_4\text{N})_2[(\text{CN})\text{AgS}_2\text{WS}_2]$	0.5	DMF	3184.5	*a*
$(n\text{-Pr}_4\text{N})_2[(\text{CN})\text{CuS}_2\text{WS}_2\text{Cu}(\text{CN})]\cdot\text{H}_2\text{O}$	0.5	DMF	2640.5	*a*
$(\text{Et}_4\text{N})_2[(\text{CN})\text{CuS}_2\text{WOS}]$	0.2	DMF	1994.3	*a*

[a] See text.

where ΔE is an average energy of electronic excitation, $\langle r^{-3}\rangle$ are appropriate radial expansion terms for the average inverse cubes of the distance of the electrons from the metal nucleus, and P_i and D_i are measures of the p- and d-electron imbalance about that nucleus. It is unlikely that the terms ΔE, P_i, and D_i are the same for species as disparate in their properties as $[\text{M}^{\text{VI}}\text{S}_4]^{2-}$ and $[\text{M}^0(\text{CO})_5\text{L}]$. For example, the ratio of the energies of the first charge-transfer bands (often taken as a measure of ΔE) is about 1 for the carbonyl derivatives[43] but 0.8–0.9 for the thiometalates (Table VI).[44] We are left with the possibility that the effects of the different terms cancel, leaving a constant ratio of 1.7, or that the gross approximations[45] introduced to produce the working equation (1) are simply not justified in the present systems. The latter seems most likely, and the fact that the ratio is essentially independent of the chemical nature of the species suggests that it is determined essentially by a nuclear property. The complexity of the diamagnetic and paramagnetic contributions to the chemical shifts and the absence of reliable theoretical methods to assess even their relative magnitudes mean that experimental examination of carefully chosen systems has a high priority at the present time.

The constant ratio of chemical shifts, on the assumption that it extends to other systems and oxidation states, is likely to be very useful for monitoring reaction mixtures for likely products and in searching for ^{183}W NMR signals, a process that can consume many hours of data accumulation. In many systems of interest, signal enhancement, e.g. by the INEPT sequence,[46] is not possible.

For rapidly rotating molecules, line widths $W_{h/2}$ for quadrupole nuclei are related[47,18b] to the square of the nuclear quadrupole coupling constant, e^2qQ/h and to the rotational correlation time of the nucleus, τ_c, by

$$W_{h/2} = \frac{3\pi}{10}\left(\frac{2I+3}{I^2(2I-1)}\right)(1 + \tfrac{1}{3}\eta^2)\left(\frac{e^2qQ}{h}\right)^2\tau_c \qquad (2)$$

where I is the nuclear spin quantum number and η the asymmetry parameter. Equation 2 implies that broad lines will be observed in general for nuclei in low-symmetry sites where the field gradient at the nucleus due to the electrons is high. In addition[48]

$$\tau_c = 4\pi a^3\eta'/3kT \qquad (3)$$

where η' is the sample viscosity, T is the absolute temperature, and a is the molecular radius of the solute molecule. Thus, decreasing the sample viscosity and increasing the temperature of measurement are expected to lead to better resolution by reducing "correlation broadening". Recently such tactics have been used with good effect to observe ^{95}Mo ($I = {}^5/_2$) NMR spectra of metal–metal-bonded species dissolved in highly viscous acid media[22] and ^{17}O ($I = {}^5/_2$) NMR of adenine nucleotides.[48]

The predominant relaxation mechanism for the ^{95}Mo nucleus in the thiomolybdates has been shown[16g] to be the quadrupolar interaction by examination of the line widths of the ^{95}Mo and ^{97} Mo resonances in H_2O. The ^{97}Mo NMR line widths were between 1 and 2 orders of magnitude greater than those of the corresponding ^{95}Mo resonances as expected from eq 2 given that the quadrupole moment eQ of ^{97}Mo is 11.1 times larger than that of ^{95}Mo.[49] The ^{95}Mo NMR line widths observed for the polynuclear thiomolybdate complexes examined in the present work (Table IX) are broader than those of the parent mononuclear thiomolybdate (at 20 °C in MeCN; in Hz): $[\text{MoS}_4]^{2-}$, <1; $[(\text{CN})\text{AgS}_2\text{MoS}_2]^{2-}$, 15; $[(\text{CN})\text{CuS}_2\text{MoS}_2]^{2-}$, 38; $[(\text{CN})\text{CuS}_2\text{MoS}_2\text{Cu}(\text{CN})]^{2-}$, 220. A 1 order of magnitude increase in line width is observed by lowering the symmetry from T_d in $[\text{MoS}_4]^{2-}$ to C_{2v} in $[(\text{CN})\text{AgS}_2\text{MoS}_2]^{2-}$, and this parallels that observed for a similar progression[16g] from $[\text{MoS}_4]^{2-}$ (0.3 Hz) to $[\text{MoO}_2\text{S}_2]^{2-}$ (2.8 Hz) in H_2O. An increased quadrupole coupling constant is responsible, although correlation broadening will make some contribution for the larger $[(\text{CN})\text{AgS}_2\text{MoS}_2]^{2-}$ anion and the presence of unresolved ^{95}Mo–^{107,109}Ag ($I = {}^1/_2$) coupling cannot be discounted. An increase in the ^{95}Mo relaxation rate caused by a rapidly relaxing neighboring quadrupolar nucleus (^{63,65}Cu, $I = {}^3/_2$) is the plausible cause of the increased line width of $[(\text{CN})\text{CuS}_2\text{MoS}_2]^{2-}$ over that of the Ag analogue (^{107,109}Ag, $I = {}^1/_2$). The cumulative effect of two neighboring copper atoms is one cause of the much greater line width of $[(\text{CN})\text{CuS}_2\text{MoS}_2\text{Cu}(\text{CN})]^{2-}$. However, the effect of correlation broadening is also important for this molecule: the line width in DMF decreases from 900 to 140 Hz upon increasing of the temperature from 20 to 100 °C (Table IX). The ^{95}Mo

---

(40) Ramsey, N. F. *Phys. Rev.* **1950**, *78*, 699.

(41) Jameson, C. J.; Gutowsky, H. S. *J. Chem. Phys.* **1964**, *40*, 1714.

(42) Mason, J. *Adv. Inorg. Chem. Radiochem.* **1979**, *22*, 199.

(43) Braterman, P. S.; Milne, G. W.; Randall, E. W.; Rosenberg, E. *J. Chem. Soc., Dalton Trans.* **1973**, 1027.

(44) The chemical shifts vary linearly with the inverse of the energy of the first charge-transfer band for $[\text{MX}_4]^{2-}$ (M = Mo, W; X = O, S, Se), but no correlations could be discerned for the species $[\text{MO}_{4-n}\text{X}_n]^{2-}$ (X = S, Se; n = 1–3).

(45) Webb, G. A. In Reference 18, Chapter 3.

(46) Brevard, C.; Schimpf, R. *J. Magn. Reson.* **1982**, *47*, 528.

(47) Abragam, A. "The Principles of Nuclear Magnetism"; Oxford University Press: London, 1961; p 314.

(48) Gerlt, J. A.; Remou, P. C.; Mehdi, S. *J. Am. Chem. Soc.* **1982**, *104*, 2848.

(49) Kidd, R. G. *J. Magn. Reson.* **1981**, *45*, 88.

NMR line widths observed for the present series of compounds are uniformly broader in DMF than in the less viscous solvent MeCN.

The line widths for the ^{183}W ($I = ^1/_2$) resonances for the limited range of binuclear and trinuclear tungsten species examined (Table IX) are rather difficult to measure accurately. The low sensitivity of the ^{183}W nucleus frequently means that only a limited number of data points define the signal after a reasonable data collection time (10–30 h for [W] = 0.5 M), and this leads to large uncertainties in line width measurement. However, the effect of the quadrupolar Cu nucleus on the ^{183}W NMR line widths (Hz) can be discerned as follows: $[WS_4]^{2-}$, <1; $[(CN)CuS_2WS_2]^{2-}$, ~5; $[(CN)CuS_2WS_2Cu(CN)]^{2-}$, ~60. Interpretation parallels that of the Mo derivatives discussed above.

Acknowledgment. The Australian Research Grants Scheme is thanked for generous support. S.F.G. thanks the Australian Wool Corp. for a research scholarship.

Registry No. $(n\text{-}Pr_4N)_2[(CN)CuS_2MoS_2]$, 86305-72-8; $(n\text{-}Pr_4N)_2[(CN)AgS_2MoS_2]$, 90790-31-1; $(n\text{-}Pr_4N)_2[(CN)CuS_2WS_2]$, 90790-29-7; $(n\text{-}Pr_4N)_2[(CN)AgS_2WS_2]$, 90790-27-5; $(Et_4N)_2[(CN)CuS_2MoS_2Cu(CN)]$, 90790-30-0; $(Ph_4As)_2[(CN)CuS_2MoS_2Cu(CN)]\cdot H_2O$, 90790-26-4; $(n\text{-}Pr_4N)_2[(CN)CuS_2MoS_2Cu(CN)]$, 86305-73-9; $(n\text{-}Pr_4N)_2[(CN)CuS_2WS_2Cu(CN)]$, 90790-33-3; $(Ph_4As)_2[(CN)CuS_2MoOS]$, 90790-35-5; $(Et_4N)_2[(CN)CuS_2MoOS]$, 90790-36-6; $(Et_4N)_2[(CN)CuS_2WOS]$, 90790-38-8; $(Ph_4P)_2[(CN)AgS_2MoS_2]$, 86430-75-3; $[MoO_4]^{2-}$, 14259-85-9; $[MoO_3S]^{2-}$, 25326-93-6; $[MoO_2S_2]^{2-}$, 16608-22-3; $[MoOS_3]^{2-}$, 19452-56-3; $[MoS_4]^{2-}$, 16330-92-0; $[MoO_3Se]^{2-}$, 90790-39-9; $[MoO_2Se_2]^{2-}$, 23507-81-5; $[MoOSe_3]^{2-}$, 39735-33-6; $[MoSe_4]^{2-}$, 21559-00-2; $[WO_4]^{2-}$, 14311-52-5; $[WO_3S]^{2-}$, 25326-94-7; $[WO_2S_2]^{2-}$, 16450-49-0; $[WOS_3]^{2-}$, 19452-55-2; $[WS_4]^{2-}$, 14916-78-0; ^{95}Mo, 14392-17-7; ^{183}W, 14265-81-7.

Supplementary Material Available: Listings of observed and calculated structure factors, anisotropic thermal parameters, and atomic coordinates and expanded listings of bond lengths and angles for I–III (Tables S1–S15) (88 pages). Ordering information is given on any current masthead page.

Contribution from the Department of Chemistry,
Baylor University, Waco, Texas 76798

Stoichiometry, Kinetics, and Mechanisms of the Chromium(VI) Oxidation of L-Cysteine at Neutral pH

DANIEL W. J. KWONG and DAVID E. PENNINGTON*

Received August 24, 1983

The stoichiometry, kinetics, and mechanisms of the chromium(VI) oxidation of L-cysteine at neutral pH have been studied. A 3:1 L-cysteine:Cr(VI) redox stoichiometry has been established, with L-cystine and $Cr(\text{L-cysteinato-}N,O,S)_2^-$ as the sole products. The rate law is of the form $-d[Cr(VI)]/dt = a[\text{L-Cys}]^2[Cr(VI)]/(1 + b[\text{L-Cys}])$, where $a = 140 \pm 13$ M^{-2} s^{-1} and $b = 220 \pm 25$ M^{-1} at 298 K, $I = 1.0$ M (Na$^+$), and pH 7.04 ± 0.02 (0.2 M $HC_2H_3O_2/NaC_2H_3O_2$). The temperature dependencies of a and b were evaluated in the range 15–35 °C. Four mechanisms are presented; however, the preferred one involves the initial formation of a chromate thio ester [$Q_1 = 220 \pm 25$ M^{-1} ($\Delta H_1 = -4 \pm 1.6$ kcal/mol, $\Delta S_1 = -1 \pm 6$ cal/(mol K))], a two-electron reduction of Cr(VI) with concomitant formation of L-cystine [$k_2 = 0.64 \pm 0.003$ M^{-1} s^{-1} ($\Delta H_2^\ddagger = 13 \pm 3.2$ kcal/mol, $\Delta S_2^\ddagger = -20 \pm 11$ cal/(mol K))], and follow-up steps to complete the stoichiometry. The results are compared with those of related studies of thiol oxidations by Cr(VI) in both acidic and neutral solutions.

Introduction

The oxidations of L-cysteine and related thiols by chromium(VI) in acidic solution have been studied by McCann and McAuley[1] and by McAuley and Olatunji.[2] Each of the oxidations is characterized by a preredox equilibrium involving the formation of a 1:1 thio ester of chromium(VI).[1,3] Both equilibrium spectrophotometric data and stopped-flow kinetic data support this mechanistic step. The rate laws for the redox processes are of the form

$$\frac{-d[Cr(VI)]}{dt} = \frac{(a[RSH] + b[H^+])[Cr(VI)][RSH]}{1 + c[RSH]} \qquad (1)$$

and involve a redox stoichiometry of [RSH]:[Cr(VI)] = 3:1 with L-cysteine in substantial excess. A mechanism utilizing the formation of the thio ester species followed by competitive redox decomposition of the intermediate by reaction with either H$^+$ or RSH was postulated to accommodate the rate law. At least two products of chromium(III) were formed in the case of L-cysteine: the first, presumably $Cr(H_2O)_4(\text{L-cystine-}N,O)^{3+}$, in ~60% yield and a more highly charged (≥4+) species in ~40% yield.

By contrast, two preliminary kinetic studies[4,5] on the oxidations of L-cysteine and other thiols at or near neutral pH indicate a simple, mixed second-order rate law. The redox stoichiometry for the oxidation of D-penicillamine[4] remains 3:1; however, the sole chromium(III) product, $Cr(\text{D-penicillaminato-}N,O,S)_2^-$, is radically different from that reported for the L-cysteine oxidation in acidic solution. A crystal structure of the closely related species $Na[Cr(\text{L-cysteinato-}N,O,S)_2]\cdot 2H_2O$ has been reported,[6] where the amino acidato groups are facially coordinated with trans sulfurs and cis nitrogens and oxygens.

In the present work a detailed kinetic and stoichiometric investigation of the oxidation of L-cysteine by chromium(VI) at neutral pH is reported.[7]

Experimental Section

Reagents. Sodium chromate and L-cysteine were used as received from Fisher Scientific Co. and U.S. Biochemical Corp., respectively. Sodium perchlorate solutions were prepared by neutralization of an aliquot of standard perchloric acid (70% Sargent-Welch) with anhydrous sodium carbonate (Mallinckrodt, AR) and diluted to volume with doubly distilled water. Solutions of perchloric acid were prepared by dilution of the stock acid with doubly distilled water. Sodium acetate (Mallinckrodt, AR) and glacial acetic acid (Du Pont, Electronic grade) were used to prepare buffer solutions to pH 7.02–7.06. $Na[Cr(\text{L-cysteinato-}N,O,S)_2]\cdot 2H_2O$ was prepared by the method of ref 6. Doubly distilled water was prepared from deionized tap water by distillation first from alkaline permanganate solution and then from

---

(1) McCann, J. P.; McAuley, A. *J. Chem. Soc. Dalton Trans.* **1975**, 783.
(2) McAuley, A.; Olatunji, M. A. *Can. J. Chem.* **1977**, *55*, 3335.
(3) McAuley, A.; Olatunji, M. A. *Can. J. Chem.* **1977**, *55*, 3328.
(4) Hojo, Y.; Sugiura, Y.; Tanaka, H. *J. Inorg. Nucl. Chem.* **1977**, *39*, 1859.
(5) Connett, P. H.; Wetterhahn, K. E. *Struct. Bonding (Berlin)*, in press.
(6) De Meester, P. Hodgson, D. J.; Freeman, H. C.; Moore, C. J. *Inorg. Chem.* **1977**, *16*, 494.
(7) The present study was well underway when a preprint of the preliminary report[5] was graciously shared by Dr. Wetterhahn.